



Research Article

Fractal Characteristics of Porosity of Electrospun Nanofiber Membranes

Ting Wang,¹ Ying Chen ,^{2,3} Wenxia Dong,¹ Yong Liu,⁴ Luoyi Shi ,¹ Rudong Chen,¹ and Tiandi Pan⁴

¹School of Mathematics Science, Tiangong University, Tianjin, China

²School of Statistics and Data Science, Naikai University, Tianjin 300071, China

³Tianjin University of Technology and Education, Tianjin 300222, China

⁴School of Textile Science and Engineering, Tiangong University, Tianjin, China

Correspondence should be addressed to Ying Chen; 18630852201@163.com

Received 8 October 2019; Revised 18 January 2020; Accepted 29 January 2020; Published 24 February 2020

Academic Editor: Samuele De Bartolo

Copyright © 2020 Ting Wang et al. This is an open access article distributed under the Creative Commons Attribution License, which permits unrestricted use, distribution, and reproduction in any medium, provided the original work is properly cited.

In this paper, the method of measuring the porosity of electrostatic nanofiber membrane by VC++ and Matlab is introduced. It is found that the ratio of the calculated porosity to the porosity measured by the mercury intrusion method accords with the famous Feigenbaum constant ($\alpha = 2.5029078750957 \dots$). The porosity distribution of nanofiber membranes was studied by VC++ and Matlab based on the image obtained by using a scanning electron microscope. The porosity distribution calculated by using a computer is magnified by e^α times which was named as relative porosity distribution. According to the relative porosity distribution, we use the algorithm proposed by Grassberger and Procaccia (briefly referred to as the G-P algorithm) to calculate the correlation fractal dimension. The correlation fractal dimension calculated from the relative porosity distribution series was between 1 and 2, consistent with geometric characteristics of coincidence samples. The fractal meaning of the Feigenbaum constant was verified again. In the end, we obtained the relationship between the associated fractal dimension and the filtration resistance by fitting in accordance with the secondary function relationship and reached the maximum correlation fractal dimension when the filtration resistance was 15–20 pa.

1. Introduction

Electrospinning is a technology of drawing polymer solution with high viscosity into fibers by electrostatic force. It can produce nanofibers with high porosity, high surface area, fine and uniform fiber, and other characteristics. Electrospinning has the following advantages: continuous fibers can be prepared directly from polymers and composites; it can be applied to a wide range of polymers; the thickness of membrane can be controlled by adjusting the collection time during the electrospun nanofiber; the dimensions and filtration feature of the electrospun nanofiber can be changed by altering the solution properties and process parameters (see [1]).

Most of the pores exist between the interior of the electrospun nanofiber membrane and the fibers. These pores

will directly affect the properties of the electrospun nanofiber membrane. At present, the methods of measuring the porosity of the electrospun nanofiber membrane include density method, image method, and mercury intrusion method (see [2–4]). However, these methods are time-consuming and costly. In recent years, more and more attention has been paid to the calculation of the porosity of electrospun nanofiber membrane by using computers (see [5, 6]). The powerful image processing ability and matrix computing ability of computers make the calculation of the porosity of electrospun nanofiber membrane simple, easy, and of low cost.

Fractal theory is a nonlinear mathematical theory derived in the middle of 1970s. The definition of fractal given by the founder Mandelbrot is that fractal is a form in which parts are in some way similar to the whole. Based on the

complexity of fiber structure in electrospinning nanofiber film, fractal can be used as an ideal mathematical research tool.

As early as the 80s of the last century, it was found by Krohn and Thompson that pores have fractal characteristic, and fractal dimension is the best description of fractal feature as the quantitative characterization and basic parameter of fractal (see [7–9]). They all look at the fractal characteristics of the pores of rocks and soils. At the beginning of the 20th century, this theory was applied to the study of electrospun nanofiber membrane. The fractal dimensions used were generally box dimensions, as given by Ai et al. (see [10, 11]). However, although the box counting method is simple and effective, it is very difficult to study the pore characteristics of electrospun nanofiber because of their obvious distribution. According to the characteristics of electrospun nanofibers, we choose the correlation fractal dimension method to study. We use the algorithm proposed by Grassberger and Procaccia to calculate its correlation fractal dimension (see [12]).

In this paper, we first give a kind of method of calculating the porosity of electrospinning nanofiber membrane by using computers. Then, according to the calculated porosity distribution sequence, using the G-P algorithm, the correlation fractal dimension of the sample is calculated and the mathematical relationship between the fractal dimension and the filtration resistance is finally discussed.

2. Preliminaries

The correlation fractal dimension calculated by the G-P algorithm is as follows:

Let us consider the system as follows:

$$\{x_k: k = 1, 2, \dots, N\}, \quad (1)$$

which is converted into a M dimensional Euclidean space, as follows:

$$X_{(M,\tau)} = \{x_n, x_{n+\tau}, \dots, x_{n+(M-1)\tau}, n = 1, 2, \dots, N\}. \quad (2)$$

First, the correlation function $C(r)$ is defined as

$$C_M(r) = \frac{1}{N(N-1)} \sum_{i \neq j} \theta(r - |X_i - X_j|), \quad (3)$$

where $\theta(x)$ is the Heaviside step function defined as

$$\theta(x) = \begin{cases} 1, & x > 0; \\ 0, & x \leq 0. \end{cases} \quad (4)$$

where $|\cdot|$ represents the distance between state vectors X_i and X_j in Euclidean space.

When r is small enough, define a constant $D(M, r)$ relative to M and r (see [10]):

$$D(M, r) = \frac{d \ln C_M(r)}{d \ln r}. \quad (5)$$

With the proper selection of M , we can find the correlation fractal dimension: Select the appropriate value of M ; when the double log curve $\ln C_M(r) - \ln r$ has a linear

interval long enough, the sample is considered to have a fractal structure. At this point, the linear slope corresponding to the linear interval is D , that is, the correlation fractal dimension of the sample.

The introduction of fractal theory and fractal methodology is of great significance in scientific methodology. Fractals are often defined as a rough or fragmented geometry that can be divided into several parts, and each part is (at least approximately) the reduced shape of the whole, i.e., having self-similar properties. Fractal and chaos are closely related; most of them are the self-organizing system, but their meanings are different. Feigenbaum, a physicist in the United States, studied the universal behavior of complex systems in detail and put forward the standard law and universality of chaotic theory (see [13]). The discovery of Feigenbaum constant ($\delta = 4.669201609103 \dots, \alpha = 1/\delta = 2.5029078750957 \dots$) reflects the order of chaotic evolution and opens the research on the universality of chaos (see [13]).

In this paper, the porosity of the electrospun nanofiber membrane calculated by Matlab software is compared with that of the electrospun nanofiber membrane obtained by the mercury intrusion method. It is found that the ratio of porosity between the two is close to the Feigenbaum constant ($\alpha = 2.5029078750957$). This feature, in a sense, reflects the fractal characteristics of the porosity distribution of the electrospun nanofiber membrane. When calculating the porosity of the electrospun nanofiber membrane, the porosity distribution is expanded to e^α multiple at first, and then, the correlation fractal dimension of the porosity distribution is calculated by using the G-P algorithm. It is found that the dimension is between 1 and 2, which is more in line with the geometric characteristics.

3. Experimental

3.1. Experimental Materials and Apparatus

3.1.1. Experimental Materials. Polyvinyl alcohol (PVA) with a relative molecule weight (Mn) of 84000 ~ 89000, alcoholysis degree of 86 ~ 89 mol%, and the average degree of polymerization 1700 ~ 1800 was purchased from Changchun Petrochemical Co., Ltd., Taiwan.

3.1.2. Experimental Apparatus. The experimental apparatuses used were as follows: DXES-01 automatic electrospinning machine, produced by Shanghai Dongxiang Nano Technology Co., Ltd.; TSI8130 Automatic Filtration Tester, from Tsai Sai Central Instrument Trade Co., Ltd. (Beijing); TM3030 Desktop Scanning Electron Microscopy, from Japan Hitachi Agency, Hitachi High-Technologies Nagano Office; and AutoPore IV 9510 high-performance automatic mercury presser, from Micromeritics Instrument Co., Ltd. (Shanghai).

3.2. Spinning Solution Preparation. Polyvinyl alcohol was dissolved in distilled water and formulated into a polyvinyl alcohol solution with a concentration of 12% (to avoid

excessive parameters, we fixed the concentration). The resulting mixed solution was stirred in a water bath at 80 C for 1 h until a homogeneous solution was formed, and then, it was statically defoamed.

3.3. Sample Preparation. At room temperature, the prepared spinning solution was poured into four 5-mL syringes with a needle diameter of 1.2 mm. From previous studies, there are five process parameters for the manufacture of electrospun nanofiber membrane as follows: 90 minutes for the spinning time; 12% for the solution concentration; the needle-to-collector distance (cm) taken as 11, 13, 15, 17, and 19; applied voltage (kV) taken as 15, 18, 20, 23, and 26; flow rate (mL/h) taken as 0.5, 0.7, 1, 1.2, and 1.5. To ensure the generality of the experiment and to avoid too many experiments, we adopted an orthogonal experiment idea and added five more experiments based on orthogonal experiment, as shown in Table 1.

The filtration resistance of each sample is tested by the TSI8310 automatic filter tester (see Table 1).

3.4. Morphological Characterization. We used the TM-3030 scanning electron microscope (SEM) of the Technology Research Center of Tianjin Polytechnic University to obtain a SEM image of the gold-sprayed sample.

4. Results and Discussion

4.1. Porosity Measurement. Current methods for measuring material porosity include nitrogen adsorption (see [14]), mercury intrusion (see [4]), impregnation (see [15]), and mass density (see [16]). The pore size of materials with pore size less than 50 nm can be measured by this nitrogen adsorption method, but it is only suitable for ultrafine powder materials. The impregnation method is a suitable test porosity method for liquid permeable nonwovens with low surface tension. However, the PVA used experimentally in this paper is a water-soluble material, so the impregnation method is not suitable for electrospinning nanofibers. Both the mercury intrusion porosimetry method and the mass density method are suitable for testing the porosity of electrospun nanofiber membrane. We tested the porosity with the mercury intrusion porosimetry at the Yanhao material laboratory in Beijing, but the test was difficult and costly, with a sample of 550 CNY. As a result, we tested only five samples: 5, 11, 19, 20, and 28. To solve the problems of high cost testing and difficult testing, a new calculation method is proposed. This method makes use of the powerful image processing ability of VC++ software and the matrix computing ability of Matlab software to process the image of electrospun nanofiber membrane. In this way, we calculated the porosity of electrospun nanofibrous membranes by an economical, simple method.

4.1.1. Threshold Segmentation. The threshold command converts gray or color images to high-contrast black and white images by specifying a certain color level as the threshold.

All pixels brighter than the threshold are converted to white, and all pixels darker than the threshold are converted to black. Scanning electron microscope image of the electrospun nanofiber membrane was read by VC++ software. Firstly, the image was transformed into a gray image, and the threshold value was adjusted according to the average grayscale value of the image to black and white images (binary images). The specific steps are as follows: running the VC++ program, preprocessing the pictures, image gray processing, binary processing, and obtaining binary black and white image, where the black part represents the nonpore part and the white part represents the pore part.

4.1.2. Calculation Using Matlab Software. For the binary black and white image after segmentation, the pixel value of each position is calculated using Matlab software and the table is generated. The porosity is the ratio of the number of white pixels to the total number of pixels, and the porosity can be calculated from the data from the table. If the porosity of the electrospun nanofiber membrane is recorded as p , then

$$p(\%) = \frac{n}{N} \times 100, \quad (6)$$

where n is the number of white pixels and N is the total number of pixels.

4.1.3. Determination of Threshold. The threshold is actually a "critical point," meaning that greater than this critical point, the threshold, is white, and the one that is less than this critical point, the threshold, is black, so there are only black and white two cases in the image. The selection of threshold is the key to the conversion of grayscale image to binary image. In this paper, we take 85% times of the average gray value of the whole image, rounded, as the image threshold, to the image binarization. The diagram before and after processing is shown in Figure 1.

4.1.4. Porosity Test Results. The measured results of the porosity of electrospun nanofiber membranes calculated by the mercury intrusion method and image processing are shown in Table 2. Table 2 shows that the ratio of porosity calculated by the mercury intrusion method and image processing method is very close to the Feigenbaum constant ($\alpha = 2.5029078750957 \dots$).

Of course, to further determine this conclusion, we also selected some samples 1, 6, 7, 21, and 2, with large differences in mean gray values for empirical evidence. When the image threshold is selected, about 85% of the average gray value of the entire image is still selected. The experimental and calculated results are shown in Table 3. The set a_1 represents the porosity of the electrospun nanofibrous membrane obtained by mercury invasion, and the set a_2 represents the porosity of the electrospun nanofibrous membrane calculated by image processing. Then, the ratio of a_1 to a_2 remains essentially consistent with the Feigenbaum constant.

TABLE 1: Experiment table.

Number of samples	Needle-to-collector distance (cm)	Applied voltage (kV)	Volume flow rate (mL/h)	The filtration resistance (pa)	Number of samples	Needle-to-collector distance (cm)	Applied voltage (kV)	Volume flow rate (mL/h)	The filtration resistance (pa)
1	11	15	0.5	11.1	16	15	20	1.5	43.1
2	13	15	0.7	22.1	17	17	20	0.5	8.5
3	15	15	1	21	18	19	20	0.7	4.9
4	17	15	1.2	11.1	19	11	23	1.2	30.1
5	19	15	1	8.9	20	13	23	1.5	29
6	19	15	1.5	6.1	21	15	23	0.5	7
7	11	18	0.5	11.5	22	17	23	0.7	5.8
8	11	18	0.7	19.3	23	17	23	1.5	7.3
9	13	18	1	15.6	24	19	23	1	9
10	15	18	1.2	19.8	25	11	26	1.5	15.7
11	17	18	1.5	9	26	13	26	0.5	9.9
12	19	18	0.5	8.1	27	13	26	1	25.9
13	11	20	1	31.2	28	15	26	0.7	8
14	13	20	1.2	27.5	29	17	26	1	5.7
15	15	20	0.7	9	30	19	26	1.2	4.3

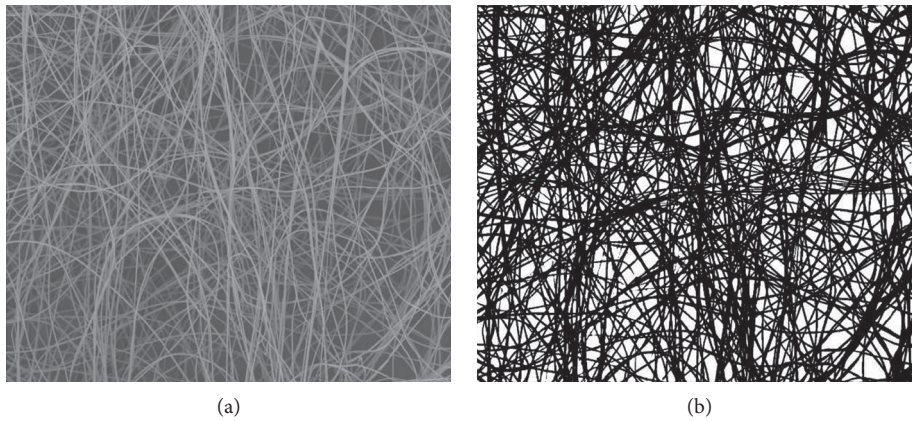


FIGURE 1: Image before and after processing.

TABLE 2: Results of porosity of the electrospun nanofiber membrane.

Number of samples	Threshold		Porosity (%)		Ratio	
	Whole-image average gray value	Image binarization selected threshold	Mercury intrusion method	Image processing	Image selection threshold/whole-image average gray value	Mercury intrusion method/image processing
5	116.357832	98	83.0	33.9032	0.8508	2.4461
11	119.866425	100	66.1	28.2820	0.8509	2.3126
19	106.131277	80	83.5	33.7828	0.8480	2.4717
20	127.836432	115	85	27.9989	0.8527	2.8793
28	115.542275	98	78.8	30.1811	0.8482	2.6109
Average					0.8501	2.5432

We believe that the measurement of porosity by the mercury intrusion method and the calculation of porosity by the image processing method should satisfy a certain relationship. The experimental results confirm that the ratio of the two is a Feigenbaum constant, which should be derived from the intrinsic structure of the electrospinning nanofibers with fractal properties, thus making their ratio more directly related to the chaotic constants. It also makes it more

convenient for us to calculate the porosity of electrospun nanofibers with computer image technology and Matlab.

It is known that with chaos, there are fractals. Only chaos emphasizes dynamic process, while fractal emphasizes geometric structure. In fact, the chaotic attractor is a fractal structure in the phase space, the fractal structure is the product of chaotic dynamics process, and the geometric convergence constant of the attractor is also a fractal

TABLE 3: Porosity of electrospun nanofiber membrane in contrast experiment.

Number of samples	Threshold		Porosity (%)		Ratio	
	Whole-image average gray value	Image binarization selected threshold	Mercury intrusion method	Image processing	Image selection threshold/whole-image average gray value	Mercury intrusion method/image processing
1	121.414597	104	83.043	34.0404	0.8565	2.4539
6	126.814396	109	86.123	33.6947	0.8595	2.5560
7	119.745632	102	85.519	35.4594	0.8518	2.4936
21	133.345346	113	86.606	37.5705	0.8549	2.3584
29	131.217394	113	89.107	33.4530	0.8535	2.6636
Average					0.8552	2.5028

dimension. Therefore, finding the physics content of universal constant of chaotic attractor is essentially the same problem as studying physical meaning of fractal dimension. Therefore, after discovering the relationship between the electrospun nanofiber membrane and the Feigenbaum constant, we further use this constant to expand the porosity distribution to the original e^α times (called it the relative porosity distribution) and to study the fractal characteristics of the structure of electrospun nanofiber membrane.

4.2. Calculation of the Correlation Fractal Dimension of Porosity Distribution

4.2.1. *Calculation of Porosity Distribution.* First, the image is processed with gray and binary using VC++ software. Second, the black and white images after binary processing are imported into the Matlab software to calculate the number of gray level of each position of the image and to generate the table. For the image of each sample, the porosity distribution of the image is obtained by measuring the proportion of porosity in the transverse coordinates of the pixel every 10 pixels (or the proportion of points whose gray value is greater than 85% of the average gray value on the line). Taking sample 3 as an example, the original image is processed, and the porosity distribution is calculated by Matlab, as shown in Figure 2: 20.8117 26.8470 29.0323 29.5525 28.5120 30.2810 28.6160 26.6389 29.7607 29.7607 29.0323 29.0323 27.5754 27.3673 28.7201 28.3039 26.5349 21.6441 23.3091 28.3039 25.7024 23.9334 29.8647 26.5349 22.2685 28.1998 28.0957 24.6618 34.1311 23.1009 27.3673 26.2227 29.1363 28.8241 25.3902 25.8065 27.9917 26.4308 24.4537 22.7888 30.1769 28.5120 28.1998 27.6795 29.6566 27.7836 29.3444 27.1592 22.1644 26.9511 24.2456 23.6212 26.9511 27.6795 30.6972 29.5525 30.2810 28.6160 19.5630 31.6337 28.3039 33.1946 28.5120 24.4537 31.7378 27.3673 28.8241 29.7607 26.3267 27.7836 29.1363 23.1009 28.5120 29.1363 28.0957 27.1592 29.2404 27.5754 30.5931 27.8876 27.5754 25.1821 26.3267 35.1717 31.9459 29.8647 33.7149 32.0499 27.4714 29.8647 28.5120 36.0042 32.9865 30.6972 33.1946 37.4610 32.7784 31.4256 33.1946 37.2529 35.4839 28.7201 35.3798 35.0676 32.9865 32.4662 32.0499 32.8824 31.2175 34.6514 35.2758 34.4433 32.9865 32.3621 27.5754 30.2810 30.3850 29.6566 28.7201 27.0552 31.0094 37.1488 15.8169 29.3444 24.0375 21.9563 31.6337 30.9053.

4.2.2. *Calculation of the Correlation Fractal Dimension.* After the porosity distribution is calculated, the correlation fractal dimension of porosity distribution is calculated by the G-P algorithm. However, we are not simply using porosity distribution data to calculate correlation fractal dimensions. In the previous section, we introduce a Feigenbaum constant associated with chaos. So, when we calculate the correlation fractal dimension of the porosity distribution, the porosity distribution data are enlarged by e^α times and the correlation fractal dimension obtained in this way accords with its geometric characteristics between 1 and 2 (see Table 4).

4.3. *Filtration Resistance Test.* The TSI8310 automatic filter tester is used to test the filtration resistance of each sample (see Table 1).

4.4. *Relationship between the Correlation Fractal Dimension of Porosity Distribution and the Filtration Resistance of Electrospun Nanofiber Membrane.* The porosity of electrospun nanofiber membrane has an extremely important influence on the filtration performance of electrospun nanofiber membrane (see [17]). The porosity distribution of electrospun nanofiber membrane has fractal characteristics, and generally speaking, the complicated microstructure can be studied by fractal theory. So, we had researched that the correlation fractal dimension of porosity is related to the filtration performance. We fitted the experimental data (Table 1) and the calculated correlation fractal dimension (Table 4) by Matlab. It was found that there was a quadratic function relationship between the correlation fractal dimension of porosity distribution and the filtration resistance. Here, the quadratic function relation is

$$y = 0.000834818733652098x^2 + 0.0313732097764176x + 1.26579722242935. \tag{7}$$

F test calculated that $F = 12.4165091855022$; look at the F test table and know that $F_{0.99}(2, 27) = 6.48851$ (see Table 5). Therefore, the quadratic function relationship between the correlation fractal dimension of porosity distribution and the filtration resistance is extremely significant.

The fitting diagram is shown in Figure 3. From Figure 3, we can see that when the filtration resistance is 15–20 pa, the

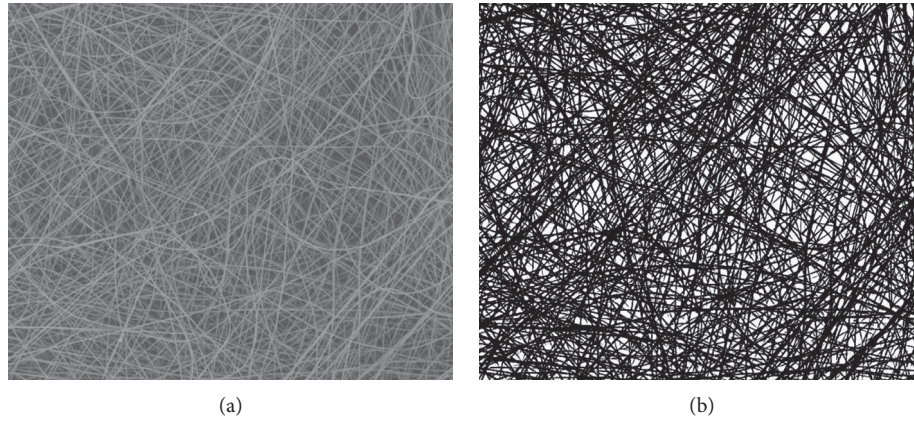


FIGURE 2: (a) Grayscale image. (b) Binary image.

TABLE 4: Correlation fractal dimension of the porosity distribution.

Number of samples	Correlation fractal dimension	Straight line intercept	Correlation coefficient	F test	Collinear interval left-end point	Collinear interval right-end point	M value
1	1.56139686172	-9.8763242714585	0.97572039	10247.6407	301	557	10
2	1.38839671912	-8.3838786693477	0.96888635	3705.6886	264	384	36
3	1.44812324781	-8.945075864163	0.98810103	15777.7817	278	469	35
4	1.4315907248	-8.3576487968196	0.95253119	1986.5803	261	361	34
5	1.4846835618	-9.4652715877316	0.97047590	6837.0920	387	596	14
6	1.58022407525	-10.491951920014	0.95075924	2934.8740	623	776	23
7	1.33696289787	-8.4468109385468	0.95156398	3536.2426	393	574	15
8	1.55601201630	-9.3009103192696	0.92082875	1407.3325	289	411	17
9	1.62172150467	-9.797105817880	0.94754834	1842.6480	339	442	45
10	1.69049555394	-10.436913933398	0.96850045	7163.9328	239	473	16
11	1.39038706342	-8.1930399219638	0.92011168	1209.3348	280	386	26
12	1.43218883519	-8.8340433166209	0.97796717	7678.9222	242	416	12
13	1.35997149018	-8.2296202827107	0.92136516	2648.0441	249	476	20
14	1.61659512319	-9.391379672001	0.90790099	995.6459	249	351	22
15	1.35311753723	-8.0186328299234	0.94924793	2225.7320	267	387	13
16	1.02169015267	-6.1646549547954	0.94651734	1840.5557	338	443	40
17	1.50027056401	-8.8875693433643	0.92285285	992.8661	308	392	20
18	1.4409252032	-9.0887640173833	0.97236387	7177.6416	330	535	10
19	1.54486251839	-9.1404089326107	0.93143693	1181.9048	302	390	33
20	1.50943945985	-8.8179988551138	0.90004084	819.3718	257	349	20
21	1.39264037832	-9.1939612974754	0.96590318	10339.8107	380	746	11
22	1.32247337693	-8.0590456568434	0.95292453	3906.8002	269	463	10
23	1.41210304077	-8.5260610755409	0.95869219	3202.7729	208	347	9
24	1.55990236576	-9.6005829927966	0.95863387	3267.5858	343	485	15
25	1.66255509007	-10.142526043924	0.94636998	2099.9066	341	461	21
26	1.41933998306	-9.2910837497103	0.97327046	6590.5368	304	486	12
27	1.55758791438	-9.4910847598210	0.98852764	15251.3988	239	417	9
28	1.44789169077	-8.7761030513857	0.9733818	3876.2389	253	360	18
29	1.59986009698	-10.023238276336	0.95830634	4321.0791	356	545	11
30	1.42842868531	-8.9589363493934	0.93127739	1395.7789	453	557	36

TABLE 5: F test table.

Source of variance	Sum of squares	Degrees of freedom	Square	F	Conspicuousness
Regression	SSR	2	SSR/2	12.4165092	Extremely significant
Residual error	SSE	27	SSE/27		
Sum	Lyy	29			

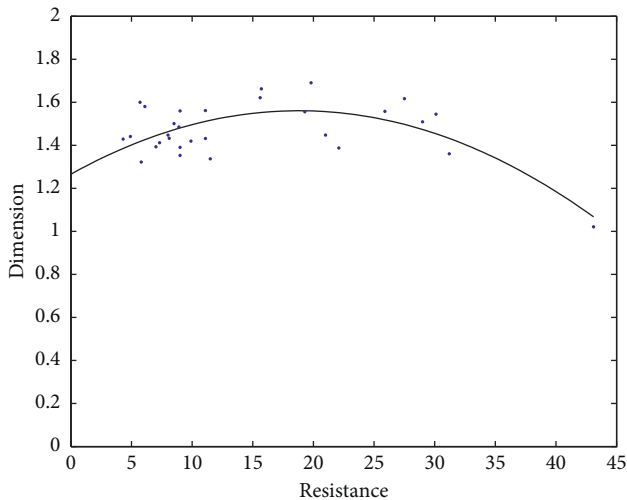


FIGURE 3: Relation between the correlation fractal dimension and the filtration resistance.

correlation fractal dimension of porosity distribution is maximum.

5. Conclusion

In this paper, the porosity using the mercury intrusion method and that calculated using the image processing method are compared. It was found that the ratio of porosity between the two was very close to the Feigenbaum constant ($\alpha = 2.5029078750957 \dots$). Secondly, the correlation fractal dimension of the electrospun nanofibrous membrane treated with the Feigenbaum constant (expansion e times) is between 1 and 2 (more consistent with its geometric characteristics). Finally, through regression analysis, we use Matlab software to prove the relationship between the related fractal dimension and the filtration resistance. The quadratic function relationship between them is very significant. It is known that the correlation fractal dimension is maximum when the filtration resistance is 15–20 pa.

Note. This result is similar to the relationship between fractal dimension and the filtration resistance of the spatial distribution of electrospinning nanofibers membrane in reference [18].

Data Availability

All the data used to support the findings of this study are included within the supplementary information files.

Conflicts of Interest

The authors declare that there are no conflicts of interest.

Authors' Contributions

Ting Wang and Ying Chen contributed equally to this work.

Acknowledgments

This research was supported by the NSFC Grant (no. 11071279), the Science and Technology Plans of Tianjin (no. 15PTSYJC00230), and Scientific Research Project of Tianjin Municipal Education Commission (no. 2019ZD01).

Supplementary Materials

Samples 1–5 are the original data selected every 10 times and are also the data group that we actually use to calculate the dimensionality; samples 6–30 are the original full data. (*Supplementary Materials*)

References

- [1] W.-E. Teo, R. Inai, and S. Ramakrishna, "Technological advances in electrospinning of nanofibers," *Science and Technology of Advanced Materials*, vol. 12, no. 1, pp. 1–19, 2011.
- [2] P. Jignesh, W. Mark, and R. Jeffrey, "Historical and future challenges with the vibrated bulk density test methods for determining porosity of calcined petroleum coke," in *Light Metals*, pp. 925–930, Springer, Cham, Switzerland, 2011.
- [3] O. Akkoyun, S. N. Ergene, K. Ciftci, and S. Yalvac, "The porosity estimation of porous basalts by using image processing methods," in *Proceedings of the 24th International Mining Congress of Turkey, IMCET*, pp. 845–849, Antalya, Turkey, April 2015.
- [4] X. Fang, Y. Cai, and D. Liu, "A mercury intrusion porosimetry method for methane diffusivity and permeability evaluation in coals: a comparative analysis," *Applied Sciences-Basel*, vol. 8, no. 6, pp. 1–16, 2018.
- [5] R. Ziel, A. Haus, and A. Tulke, "Quantification of the pore size distribution (porosity profiles) in microfiltration membranes by SEM, TEM and computer image analysis," *Journal of Membrane Science*, vol. 323, no. 2, pp. 241–246, 2008.
- [6] Y. Chen, N. Deng, B.-J. Xin, W.-Y. Xing, and Z.-Y. Zhang, "Nonwovens structure measurement based on NSST multifocus image fusion," *Micron*, vol. 123, Article ID 102684, 2019.
- [7] C. E. Krohn and A. H. Thompson, "Fractal sandstone pores: automated measurements using scanning-electron-microscope images," *Physical Review B*, vol. 31, no. 9, pp. 6366–6374, 1986.
- [8] G. Grigorov, Y. G. Zaynulin, and G. P. Shveykin, "Fractal analysis of fracture of powder metallurgical hard alloy," *Inorganic Materials: Applied Research*, vol. 8, no. 1, pp. 67–74, 2017.
- [9] B. M. Yu, L. J. Lee, and H. Q. Cao, "Fractal characters of pore microstructures of textile fabrics," *Fractals*, vol. 9, no. 2, pp. 55–62, 2007.
- [10] T. Ai, R. Zhang, H. W. Zhou, and J. L. Pei, "Box-counting methods to directly estimate the fractal dimension of a rock surface," *Applied Surface Science*, vol. 314, pp. 610–621, 2014.
- [11] A. Manning and K. Simon, "Dimension of slices through the sierpinski carpet," *Transactions Of The American Mathematical Society*, vol. 365, no. 1, pp. 213–250, 2012.
- [12] P. Grassberger and I. Procaccia, "Measuring the strangeness of strange attractors," *Physica D Nonlinear Phenomena*, vol. 9, no. 1, pp. 189–208, 1983.
- [13] M. J. Feigenbaum, "Quantitative universality for a class of nonlinear transformations," *Journal of Statistical Physics*, vol. 19, no. 1, pp. 25–52, 1978.

- [14] N. Gao, K. Chen, and Q. Cui, "Development of CaO-based adsorbents loaded on charcoal for CO₂ capture at high temperature," *Fuel*, vol. 260, no. 15, pp. 1–10, 2020.
- [15] Z. Jin, R. Hu, H. Wang, J. Hu, and T. Ren, "One-step impregnation method to prepare direct Z-scheme LaCoO₃/g-C₃N₄ heterojunction photocatalysts for phenol degradation under visible light," *Applied Surface Science*, vol. 491, pp. 432–442, 2019.
- [16] H.-T. Wang, J.-Q. Jia, and X.-H. Li, "Cranny density parameters and porosity measured by elastic wave method in quasi-isotropic cranny rock masses," *Journal of Central South University of Technology*, vol. 13, no. 5, pp. 598–602, 2006.
- [17] C. Ma, Y. Wu, and J. Y. Yu, "Investigation on the relation between structure of PBS electrospinning nonwovens and filtration properties," *Technical Textiles*, vol. 26, no. 5, pp. 13–15, 2008.
- [18] Y. Chen, L. Qi, L. Zhang, R. Zhu, and R. Chen, "Study of fractal dimension of electrospun nanofibres non-woven fabrics and the relationship between it and air resistance," *Journal of Innovative Technology and Education*, vol. 2, no. 1, pp. 15–28, 2015.